Title: Reconstitution of *Spiroplasma* swimming by expressing two bacterial actins in synthetic minimal bacterium

Authors: Hana Kiyama[1], Shigeyuki Kakizawa[2], Yuya Sasajima[1], Yuhei O Tahara[1,3], Makoto Miyata[1,3]*

Affiliations:

[1]Graduate School of Science, Osaka City University, 3-3-138 Sugimoto, Sumiyoshi-ku, Osaka 558-8585, Japan.

[2]Bioproduction Research Institute, National Institute of Advanced Industrial Science and Technology, Tsukuba, Japan.

[3]The OCU Advanced Research Institute for Natural Science and Technology (OCARINA), Osaka City University, 3-3-138 Sugimoto, Sumiyoshi-ku, Osaka 558-8585, Japan.

*Corresponding author. Email: miyata@osaka-cu.ac.jp

Abstract: Motility is one of the most important features of life, but its evolutionary origin is still unknown. Here, we focus on *Spiroplasma*, commensal or parasitic bacteria. They swim by the helicity switching of a ribbon-like cytoskeleton composed of six proteins each evolved from a nucleosidase and a bacterial actin called MreB. We expressed these proteins in a synthetic minimal bacterium, JCVI-syn3B whose genome was computer-designed and chemically synthesized. The synthetic bacterium showed swimming motility with the features common with *Spiroplasma* swimming. Moreover, some combinations of two proteins showed helical cell shape and swimming, suggesting that the swimming was originated from differentiation and coupling of the bacterial actin.

One-Sentence Summary: Expression of two bacterial actins gave cell helicity and swimming to a synthetic minimal cell.

Motility is observed in many forms of life, and is arguably one of the major determinants for survival. If we focus on the force-generating units of cell motility, all cell motilities reported so far can be classified into 18 mechanisms (*1*). Generally, the direct evolutional ancestor of the individual mechanisms cannot be identified, probably because many of these have been in existence for a long time. However, it is possible to discuss the origins and their evolution. Cell motility is thought to originate from the movements of housekeeping proteins after they were amplified and transmitted to cell outside. However, this process has not been experimentally demonstrated. class Mollicutes are parasitic or commensal bacteria, characterized by a small genome (*2, 3*). Interestingly, there are three unique motility mechanisms in class Mollicutes (*4-6*). It is likely that when phylum Firmicutes evolved to stop peptidoglycan synthesis in order to escape the host's immune system, they also stopped flagellar motility, which depends on the peptidoglycan layer, and then acquired unique motility (*1, 5*). In one of the three types of motilities, *Spiroplasma* swimming, they push water backwards by switching the handedness of their helicity (*4, 7-9*). These schemes are completely different from those of the spirochete, a group of bacteria whose cells are also helical. The helical shape of *Spiroplasma* is likely determined by a ribbon-like cytoskeleton, which is consist of mainly fibrils evolved from nucleosidases (*10-12*) and five classes of *Spiroplasma* MreBs evolved from MreB, the bacterial actin (*12-15*). Here, we call *Spiroplasma* MreBs as SMreBs, because they are distantly related to MreBs found in walled-bacteria (*13, 16, 17*). The helicity of ribbon is determined by fibril protein, but the mechanism of helicity switching is unknown.

A synthetic bacterium JCVI-syn3.0B (syn3B in short), was established by J. Craig Venter Institute (JCVI) in 2016, as a combination of a cell of *Mycoplasma capricolum* and a genome designed based on *Mycoplasma mycoides*. Both *Mycoplasma* species belong to *Spiroplasma* clade, one of four Mollicutes clades. It has a fast growth rate beneficial for genome manipulation, a roughly spherical morphology, and no motility (*18, 19*). In this study, we reconstituted *Spiroplasma* swimming in syn3B by adding seven genes and identified the minimal gene set for *Spiroplasma* cell helicity and swimming.

Results

Reconstitution of *Spiroplasma* swimming in syn3B. We focus on *Spiroplasma eriocheiris*, an actively swimming pathogen of crustaceans (*14*). Seven genes which are likely related to swimming are encoded in four loci in the genome, comprising fibril, five classes of SMreB, and a non annotated conserved gene. We assembled these genes into a 8.4 kb DNA fragment and incorporated it into the syn3B genome, using the Cre*/loxP* system (Fig. 1A, Fig. S1, Table S1) (*20, 21*). An active promoter of syn3B, Ptuf was inserted at the upstream of the gene cluster. Surprisingly, under optical microscopy 48% of the syn3B cells showed filamentous cell shape and active movements, presumably accompanied by force generation, and moreover 13% had helical shape and swimming motility (Fig. 1B, Movie S1). Then, we named this construct as syn3Bsw. The width and pitch of the cell helices analyzed with light microscopy were slightly different from those of *Spiroplasma* cells (Fig. 1C). If we focus on cells that are partially bound to the glass, we can see that a free part of cell was rotating with some reversals (Fig. 1D, Movie S2), meaning that helicity switching causes the helix rotation in syn3Bsw, like *Spiroplasma* swimming. Next, we analyzed the helices and their handedness of cell images in each frame of swimming video (Fig. 1E, F). The handedness of the cell helix was different depending on the axial position, and the helicity changed with time. Then, we measured the movement and rotation speed of the helix from the part where the helix appeared to move along the cell axis

smoothly. The helix movement and rotation speeds were 8.2 ± 3.7 μm/s and 11.6 ± 4.8 /s (n=10) for syn3sw, not significantly different from 8.8 ± 2.8 μm/s and 12.0 ± 3.6 /s (n=16) for *Spiroplasma*. In the cryo-electron microscopy (EM) image of syn3Bsw cells, fi1aments running along the axis were observed in the inner part of the curvature, like *Spiroplasma* cells (Fig. S2). The filaments recovered from syn3Bsw cells showed periodicity and width, that were similar to fibril filament from *Spiroplasma* cells (Fig. 1G, Fig. S3)(*10*). In addition, electrophoretic and mass spectrometric analyses of cell lysates showed that fibril and all SMreBs were expressed in syn3sw cells (Fig. S4, Table S2). These results show that the expression of *Spiroplasma* proteins inside syn3Bsw cells resulted in the formation of internal filaments that reconstituted helical shape, helicity switching, and swimming.

Differences in swimming between syn3Bsw and *Spiroplasma.* The speeds of helix movement and rotation were not significantly different between syn3Bsw and *Spiroplasma* (Fig. 1F). However, the trajectory of the cells over 10 s showed that syn3Bsw could not travel long distances, unlike *Spiroplasma* (Fig. 1H). The reason can be seen in the time course of helicity switching, showing little continuity in the rotation that hampers long distance traveling (Fig. 1F). This may be caused by lack of cooperativity in the helicity switching generating the helix rotation. EM images of syn3Bsw cells did not show the tapered pole including an inner architecture called “dumbbell”, unlike *Spiroplasma* cells (Fig. 1I)(*14*), suggesting that the tapered pole made by unknown proteins have some roles for continuous helicity switching of the ribbon.

Role of component proteins. To examine the role of each protein, we made and analyzed constructs in which each protein was not expressed (Fig. 2, A and B, Movie S3). In order not to affect gene expression by the change in the DNA and RNA structures, we introduced nonsense mutations to one of the 8th-22nd codons of each structural gene (Fig. S1). We confirmed by electrophoresis that the target proteins were no longer expressed in the mutant cells (Fig. S5). No significant differences from syn3Bsw were observed in cell structures and behaviors for five of the six constructs (Fig. 2A). However, in the construct missing SMreB5, the helix width was 0.64 ± 0.13 μm, significantly larger than that of syn3Bsw, in half of the filamentous cells, and the cells moved but did not swim. The distinctive features by the lack of SMreB5 are consistent with a previous observation that *Spiroplasma citri* lost helicity and swimming by the lack of SMreB5 (*13*). These results suggest that the seven proteins have redundant roles for helix formation and swimming.

We then examined syn3B constructs expressing each protein (Fig. 2C, Movie S4). The cells expressing only fibril protein formed helical cell shape with a pitch of 0.72 ± 0.08 μm and a width of 1.0 ± 0.10 μm, which is wider than *Spiroplasma* cells. The pitch of the helix is in good agreement with the number from isolated fibrils, which is consistent with the fact that fibril is the major component of the ribbon (*10, 11*). The cells expressing SMreB2 formed filamentous morphology, and some of them formed helices with variety of pitches as 0.66 ± 0.12μm. The cells expressing only SMreBs1, 3, or 4, did not show difference in cell shape from the original syn3B.

Expressing pair of SMreBs. Next, we analyzed the shapes and behaviors of cells expressing ten combinations of SMreB protein pairs (Fig. 3A, Fig. S1). As five classes of SMreB can be divided into three groups from amino acid sequence: 5-2, 4-1, and 3 (*13, 16, 17*), here we will discuss the

results based on this classification. In the pairs of SMreBs selected from each of the 5-2 and 4-1 groups, surprisingly, the cells in the 5-1 and 5-4 combinations showed helix formation and movements, and some cells showed swimming like syn3Bsw, with occurrence frequencies comparative to syn3Bsw (Fig. 3, B and C, Movie S5). The cells of 2-1 showed filamentous morphology and movements. The cells of 2-4 combination showed filamentous morphology but basically immotile. However, a few in several hundred cells showed movements. In the combinations of one in 5-2 or 4-1 groups paired with 3, cells of 3-2 formed right-handed helix (Fig. 3D, Movie S6). In the combinations of 3-1, 3-4 and 3-5, the cells did not show differences from the original syn3B. In the combinations in the same group, 5-2 and 4-1 cells were filamentous, and 4-1 cells rarely formed a short, right-handed helix.

In the construct of 5-4, we fused a fluorescent protein mCherry into SMreB 5 and 4 at a position suggested by previous studies (Fig. 3E, Fig. S1, Movie S7)(*22*). The cells expressing SMreB5 fused with mCherry showed a helical cell shape and swimming as observed in the 5-4 cells. Fluorescence was observed throughout a cell, suggesting that SMreB5 filaments were formed along the entire cell axis. Also this result showed that the mCherry fusion did not interfere the functions of SMeB5. The 5-4 cells with mCherry fusion to SMreB4 did not show helicity basically. Even helical cells found in hundreds of cells did not show any movements. To clarify the roles of fibril, a major component of ribbon structure, we analyzed cells expressing fibril additionally to SMreBs 4 and 5 (Fig. 3F, Movie S8). The differences between presence and absence of fibril protein were subtle in analyses conducted in this study.

Discussion

MreB belonging to actin superfamily, forms a short antiparallel double-strand filament, based on ATP energy (*23, 24*). It has the ability sensing the curvature of the peripheral structures and serves to guide the bacterial peptidoglycan synthase to the positions required for the synthesis (*25*). Isolated SMreBs also form fibers similar to those of MreB (*13, 26*). Our results indicate that the helix formation and force generation of *Spiroplasma* occur by the interaction between different SMreBs. The mechanism can be explained as follows (Fig. 4). Protofilaments made of proteins belonging to either SMreB 5 and 2 or 4 and 1 group are aligned along the cell axis, and are bound together. If the unit length in each protofilament is different, some curvature is induced in the double strand, resulting in helix formation. If these protofilaments undergo a local length change at different timing using ATP energy, the curvature changes like a Bi-metallic strip resulting in helicity switching (*4*). The length change may be related to polymerization and depolymerization in terms of the change in axial distance between subunits. Remarkably, the difference in amino acid sequence between SMreBs 5-2, and 4-1 in *S. eriocheiris* is only less than 34% (*16*). This small number of differences suggest that the ancestors of SMreB may have acquired stability, helicity, and switching after accidental acquisition of different properties. In other words, it may represent the moment when a small structural change in a housekeeping protein is amplified by an accidental accumulation of mutations, leading to motility. The reason for the existence of as many as five SMreBs, even though two proteins are capable of acquiring helicity and force generation, is unclear. It may be advantageous for efficient and robust swimming, possibly in different environments, or for chemotaxis. The participation of fibril can be explained in a similar way.

Here, we used JCVI-syn3B as an experimental platform (*18, 19*). Since the genes of synthetic bacteria are derived from organisms related to *Spiroplasma*, it remains possible that factors

derived from synthetic bacteria, such as proteins and membrane structures, are essential for the helix formation and swimming. Then, it is still a future challenge to elucidate the mechanism of *Spiroplasma* swimming completely. Nevertheless, the results of this study demonstrate that syn3B is a good system to study cell evolution.

Materials and Methods

Bacterial strains and culture conditions. JCVI-syn3B (GenBank: CP069345.1), *Spiroplasma eriocheiris* (TDA-040725-5T), *Escherichia coli* (DH5α) for DNA manipulation were cultured in SP4 (*18, 19*), R2 (*14, 27*), and LB media, respectively. Cultures at an optical density 0.03 at 620 nm were used for analyses of JCVI-syn3B and *Spiroplasma eriocheiris*. Transformation of JCVI-syn3B was performed as previously described (*21*).

Plasmid construction. The *Spiroplasma* genome was isolated as previously described (*27*). The plasmid used to transform JCVI-syn3B to obtain syn3Bsw (pSeW001) were constructed as follows (Fig. S1). Focused *Spiroplasma* DNA regions, *puroR* gene, and vector fragment were amplified from the *Spiroplasma* genome DNA and pSD079 DNA (*21*) as five PCR products, using primer sets listed in Table S1. The DNA fragments were assembled by In-Fusion® HD Cloning Kit (Takara Bio Inc. Kusatsu, Japan). pSeW002 was constructed by replacing the upstream region of the 1st gene, *fibril* in pSeW001 to Ptuf fragment (promoter from the EF-Tu gene) amplified from pSD079. pSeW102, pSeW202, pSeW302, pSeW402, pSeW502, pSeW602, and pSeW702 were modified to introduce nonsense mutation in individual genes. The plasmids to construct other strains were modified from pSeW005, which was constructed by the process stated above, using pSeW002 as the PCR template. Ptuf or Pspi (Spiralin promoter from *Spiroplasma*) (*21*) were inserted at the 5' end of the 1st *orfs*. All DNA fragments were verified for DNA sequence.

Protein analyses. Profiling and identification of protein in cells were performed as previously described (*14, 28, 29*).

Phase-contrast and fluorescence microscopy. The cultured cells of *Spiroplasma* and syn3B were observed in 0.5 × SP4 medium diluted by PBS, containing 0.5% methylcellulose and 0.5 mg/mL BSA. The cell density was adjusted by centrifugation at 11, 000 × g for 10 min, followed by suspension with the diluted medium. The cell suspension was inserted into a tunnel slide (*14, 27, 30, 31*) and observed by an inverted microscope IX71 (Olympus, Tokyo, Japan) equipped by UPlanSApo 100× 1.4 NA Ph3 and a CMOS (complementary metal-oxide-semiconductor) camera, DMK33UX174 (The Imaging Source Asia Co., Ltd. Taipei, Taiwan). The videos were analyzed by ImageJ ver.1.53f51 (Fiji) using plugins, MTrackJ and EGT (Empirical Gradient Threshold), and a color foot printing macro (*32*).

Electron microscopy. To observe the intact cells, cultured cells were collected by the centrifugation, suspended to be 10-fold density of the original in the medium, and fixed using 0.5% glutaraldehyde for 5 min at 25°C. After quenching by 500 mM Tris-HCl pH7.5, the cells were collected by the centrifugation, washed and suspended in PBS to be 40-fold density of the original. The cell suspension was placed on a carbon-coated grid for 5 min, removed, rinsed by PBS three times, and then stained with 2% phosphotungstic acid for 60 s. To observe the internal structure, the cell suspension was treated with PBS including 0.1 mg/mL DNase, 1 mM $MgCl_2$

and 1mM PMSF (phenylmethylsulfonyl fluoride) for 10 min at 4°C, and centrifuged at 200,000 × g for 30 min at 4°C. The pellet was suspended in PBS to be 160-fold density of the original, placed on the EM grid for 2 min, and stained with 2% phosphotungstic acid for 60 s. The images were acquired using a JEM1010 EM (JEOL, Akishima, Japan) equipped with a FastScan-F214(T) CCD (charged-coupled device) camera (TVIPS, Gauting, Germany). For cryoEM, the cultured cells were collected and suspended to be 10-fold density of the original and frozen as described previously (*33*). The images were captured by Talos F200C EM (Thermo Fisher Scientific, Waltham, USA) equipped by 4k × 4k Ceta CMOS camera (Thermo). The images were analyzed using the ImageJ.

References and Notes

1. M. Miyata *et al.*, Tree of motility - A proposed history of motility systems in the tree of life. *Genes Cells* **25**, 6-21 (2020).
2. H. Grosjean *et al.*, Predicting the minimal translation apparatus: lessons from the reductive evolution of mollicutes. *PLoS Genet* **10**, e1004363 (2014).
3. S. Razin, L. Hayflick, Highlights of mycoplasma research--an historical perspective. *Biologicals* **38**, 183-190 (2010).
4. Y. Sasajima, M. Miyata, Prospects for the mechanism of *Spiroplasma* swimming. *Front Microbiol* **12**, 706426 (2021).
5. M. Miyata, T. Hamaguchi, Integrated information and prospects for gliding mechanism of the pathogenic bacterium *Mycoplasma pneumoniae*. *Front Microbiol* **7**, 960 (2016).
6. M. Miyata, T. Hamaguchi, Prospects for the gliding mechanism of *Mycoplasma mobile*. *Curr Opin Microbiol* **29**, 15-21 (2016).
7. D. Nakane, T. Ito, T. Nishizaka, Coexistence of two chiral helices produces kink translation in *Spiroplasma* swimming. *J Bacteriol* **202**, e00735-00719 (2020).
8. H. Wada, R. R. Netz, Hydrodynamics of helical-shaped bacterial motility. *Phys Rev E Stat Nonlin Soft Matter Phys* **80**, 021921 (2009).
9. J. W. Shaevitz, J. Y. Lee, D. A. Fletcher, *Spiroplasma* swim by a processive change in body helicity. *Cell* **122**, 941-945 (2005).
10. Y. Sasajima, T. Kato, T. Miyata, K. Namba, M. Miyata, Elucidation of fibril structure responsible for swimming in *Spiroplasma* using electron microscopy. *bioRxiv*, 10.1101/2021.1102.1124.432793 (2021).
11. S. Cohen-Krausz, P. C. Cabahug, S. Trachtenberg, The monomeric, tetrameric, and fibrillar organization of Fib: the dynamic building block of the bacterial linear motor of *Spiroplasma melliferum* BC3. *J Mol Biol* **410**, 194-213 (2011).
12. J. Kürner, A. S. Frangakis, W. Baumeister, Cryo-electron tomography reveals the cytoskeletal structure of *Spiroplasma melliferum*. *Science* **307**, 436-438 (2005).
13. S. Harne *et al.*, MreB5 Is a determinant of rod-to-helical transition in the cell-wall-less bacterium *Spiroplasma*. *Curr Biol* **30**, 4753-4762.e4757 (2020).
14. P. Liu *et al.*, Chemotaxis without conventional two-component system, based on cell polarity and aerobic conditions in helicity-switching swimming of *Spiroplasma eriocheiris*. *Front Microbiol* **8**, 58 (2017).
15. S. Trachtenberg *et al.*, Structure of the cytoskeleton of *Spiroplasma melliferum* BC3 and its interactions with the cell membrane. *J Mol Biol* **378**, 778-789 (2008).
16. D. Takahashi, I. Fujiwara, M. Miyata, Phylogenetic origin and sequence features of MreB from the wall-less swimming bacteria *Spiroplasma*. *Biochem Biophys Res Commun* **533**, 638-644 (2020).
17. C. Ku, W. S. Lo, C. H. Kuo, Molecular evolution of the actin-like MreB protein gene family in wall-less bacteria. *Biochem Biophys Res Commun* **446**, 927-932 (2014).
18. J. F. Pelletier *et al.*, Genetic requirements for cell division in a genomically minimal cell. *Cell* **184**, 2430-2440 e2416 (2021).
19. C. A. Hutchison, 3rd *et al.*, Design and synthesis of a minimal bacterial genome. *Science* **351**, aad6253 (2016).
20. F. Nishiumi *et al.*, Blockade of endoplasmic reticulum stress-induced cell death by *Ureaplasma parvum* vacuolating factor. *Cell Microbiol*, e13392 (2021).
21. A. M. Mariscal *et al.*, Tuning gene activity by inducible and targeted regulation of gene expression in minimal bacterial cells. *ACS Synth Biol* **7**, 1538-1552 (2018).

22. J. Salje, F. van den Ent, P. de Boer, J. Lowe, Direct membrane binding by bacterial actin MreB. *Mol Cell* **43**, 478-487 (2011).
23. F. van den Ent, T. Izore, T. A. Bharat, C. M. Johnson, J. Lowe, Bacterial actin MreB forms antiparallel double filaments. *Elife* **3**, e02634 (2014).
24. D. Popp *et al.*, Filament structure, organization, and dynamics in MreB sheets. *J Biol Chem* **285**, 15858-15865 (2010).
25. H. Shi, B. P. Bratton, Z. Gitai, K. C. Huang, How to build a bacterial cell: MreB as the foreman of *E. coli* construction. *Cell* **172**, 1294-1305 (2018).
26. D. Takahashi *et al.*, Structure and polymerization dynamics of bacterial actin MreB3 and MreB5 involved in *Spiroplasma* swimming. *bioRxiv*, 10.1101/2021.1104.1107.438887 (2021).
27. N. Terahara, I. Tulum, M. Miyata, Transformation of crustacean pathogenic bacterium *Spiroplasma eriocheiris* and expression of yellow fluorescent protein. *Biochem Biophys Res Commun* **487**, 488-493 (2017).
28. T. Toyonaga *et al.*, Chained structure of dimeric F1-like ATPase in *Mycoplasma mobile* gliding machinery. *mBio*, e0141421 (2021).
29. Y. Kawakita *et al.*, Structural study of MPN387, an sssential protein for gliding motility of a human-pathogenic bacterium, *Mycoplasma pneumoniae*. *J Bacteriol* **198**, 2352-2359 (2016).
30. T. Kasai *et al.*, Role of binding in *Mycoplasma mobile* and *Mycoplasma pneumoniae* gliding analyzed through inhibition by synthesized sialylated compounds. *J Bacteriol* **195**, 429-435 (2013).
31. D. Nakane, M. Miyata, *Mycoplasma mobile* cells elongated by detergent and their pivoting movements in gliding. *J Bacteriol* **194**, 122-130 (2012).
32. Y. Hiratsuka, M. Miyata, T. Q. Uyeda, Living microtransporter by uni-directional gliding of *Mycoplasma* along microtracks. *Biochem Biophys Res Commun* **331**, 318-324 (2005).
33. M. Nishikawa *et al.*, Refined mechanism of *Mycoplasma mobile* gliding based on structure, ATPase activity, and sialic acid binding of machinery. *mBio* **10**, e02846-02819 (2019).

Acknowledgments: We thank Prof John Glass and JCVI for helpful inputs about JCVI-syn3, Ikuko Fujiwara, Takuma Toyonaga for helpful discussion, and Junko Shiomi, Tomomi Shimonaka for technical assists. **Funding:** This study was supported by JST CREST (Grant Number JPMJCR19S5) and JSPS KAKENHI (Grant Number JP21J23306). **Author contributions:** Conceptualization: HK, SK, MM, Methodology: SK, YS, Investigation: HK, YS, Visualization: HK, YS, YOT, Writing – original draft: HK, MM, Writing – review and editing: HK, SK, MM, Funding acquisition: MM, HK. Competing interests: Authors declare no competing interests. **Data and materials availability:** All data are available in the main text or the supplementary materials.

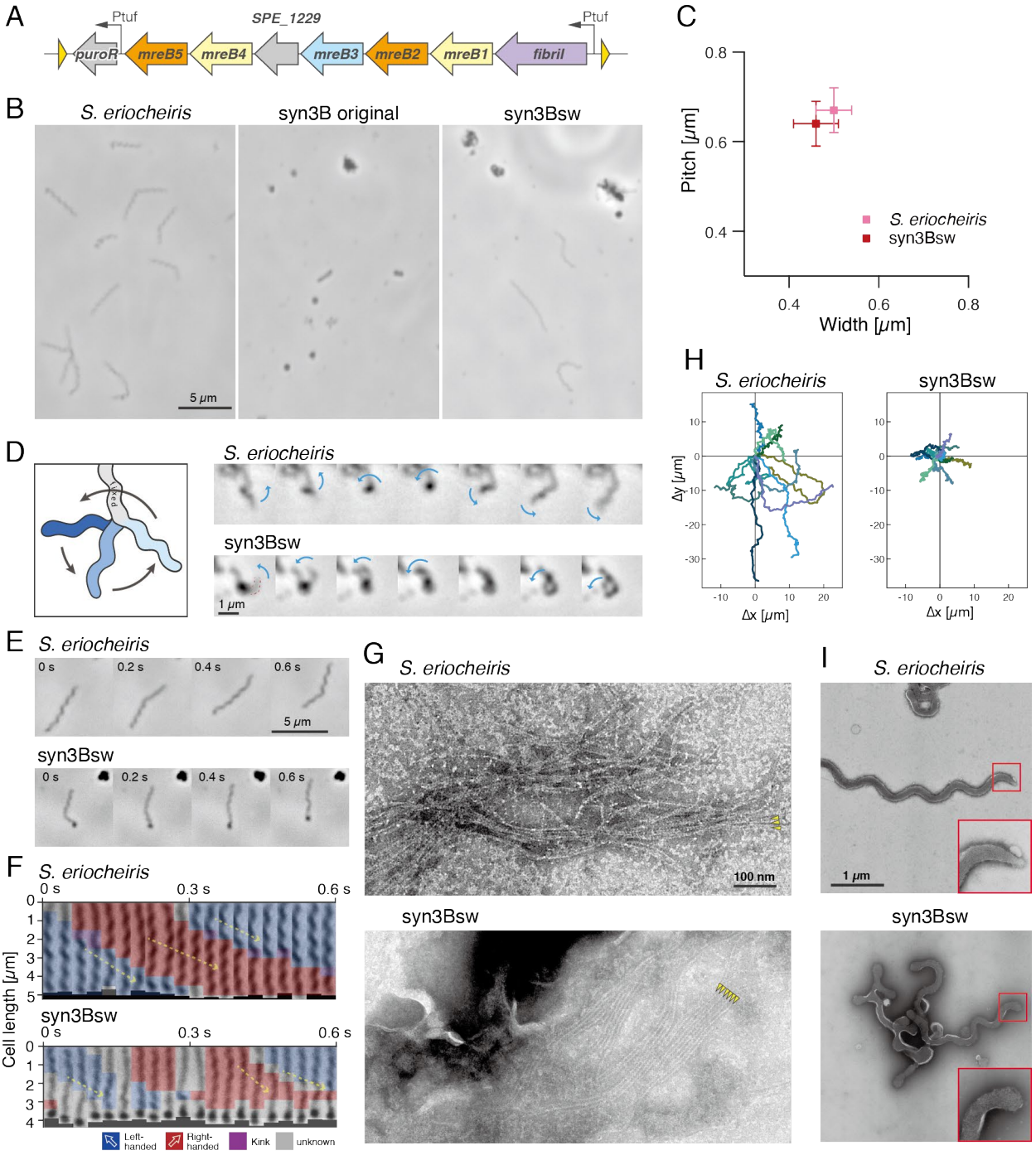

Fig. 1. Reconstitution of Spiroplasma swimming in syn3B by expressing seven genes. (**A**) A DNA fragment transferred into *loxP* site of syn3B, including seven genes from *Spiroplasma* and a puromycin resistance gene, "*puroR*". A non annotated gene, *SPE_1229* is shown by a gray arrow. Ptuf and *loxP* sites are shown by black arrows and yellow triangles, respectively. (**B**) Field cell images of three strains indicated on the top. In syn3Bsw, DNA fragment shown in (A) is inserted into the genome by Cre/*loxP* system. The cells were observed by phase contrast microscopy. (**C**) Distribution of cell helicity parameters measured by optical microscopy. (**D**)

Rotational behaviors of freely moving part of *Spiroplasma* and syn3Bsw cells. A schematic is shown in the left. The cell is fixed to the glass through the light gray part and blue part is rotating. Consecutive video frames are shown for every 0.03 s. A rotational behavior of free part is marked by blue arrows. The rotating part in syn3Bsw is marked by a red broken line. (**E**) Consecutive video frames of swimming cells for every 0.2 s. (**F**) Change in helicity analyzed for videos shown in (E). The cell images were straightened and analyzed by ImageJ, and then colored for their handedness. Smooth traveling helix is marked by a yellow arrow. (**G**) Negative-staining EM images of filaments recovered from *Spiroplasma* and syn3Bsw cells. Filaments are marked by yellow triangles. (**H**) Traces of a pole of ten cells for 10 s colored differently. (**I**) Cell images under negative-staining EM images of *Spiroplasma* and syn3Bsw cells. A cell pole is magnified as inset.

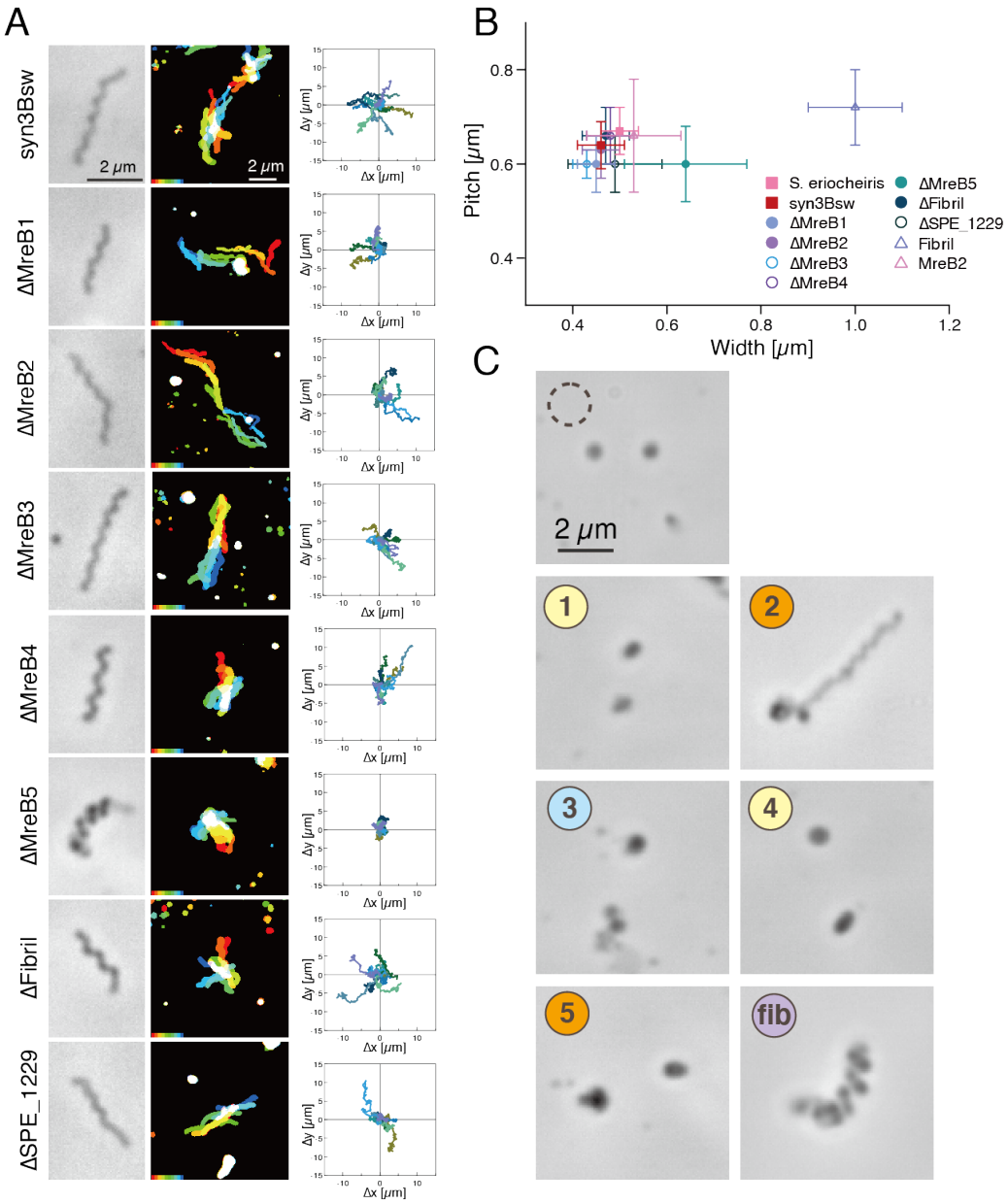

Fig. 2. Role of individual proteins in syn3 swimming. (**A**) Structure and behaviors of cells lacking one of seven proteins from syn3sw. For each construct, phase-contrast cell image (left), integrated cell images every 1 s for 10 s with colors changing from red to blue (middle), and traces of a pole of ten cells for 10 s (right) are shown. (B) Distribution of cell helicity parameters for individual constructs analyzed with optical microscopy. (C) Phase-contrast image of cells expressing single *Spiroplasma* protein marked by "fib" and number of SMreBs. The original syn3B is marked by a broken circle.

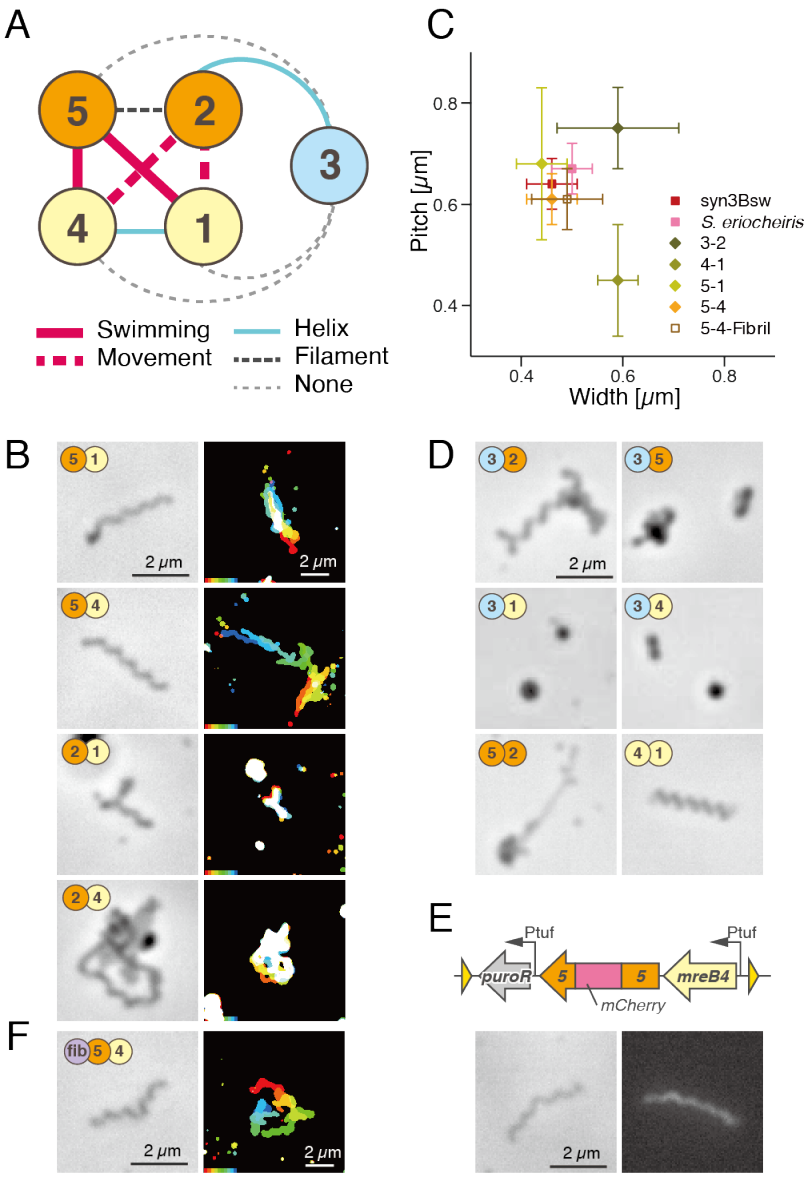

Fig. 3. Morphology and behaviors of syn3B cells expressing pair of SMreB proteins. (**A**) Schematic of SMreB combinations with protein groups. Each SMreB is presented by a numbered circle with a group color. The characters resulted in syn3B cells by gene expression are presented by line formats. (**B**) Image (left) and behaviors (right) of syn3B cells expressing pair of SMreBs. Cells of four constructs presented here showed movements. (**C**) Distribution of parameters for cell helicity. (**D**) Phase-contrast image of cells expressing other combinations of protein pairs. Six pairs did not show movements. (**E**) SMreB5 localization in cell expressing SMreB 4 and 5. Schematic of integrated genes is shown (upper). mCherry gene is inserted into C-terminal side of tyrosine residue at 218th position. Phase-contrast and fluorescence images are shown (lower). (**F**) Image (left) and behaviors (right) of syn3B cells expressing SMreBs 4, 5, and fibril.

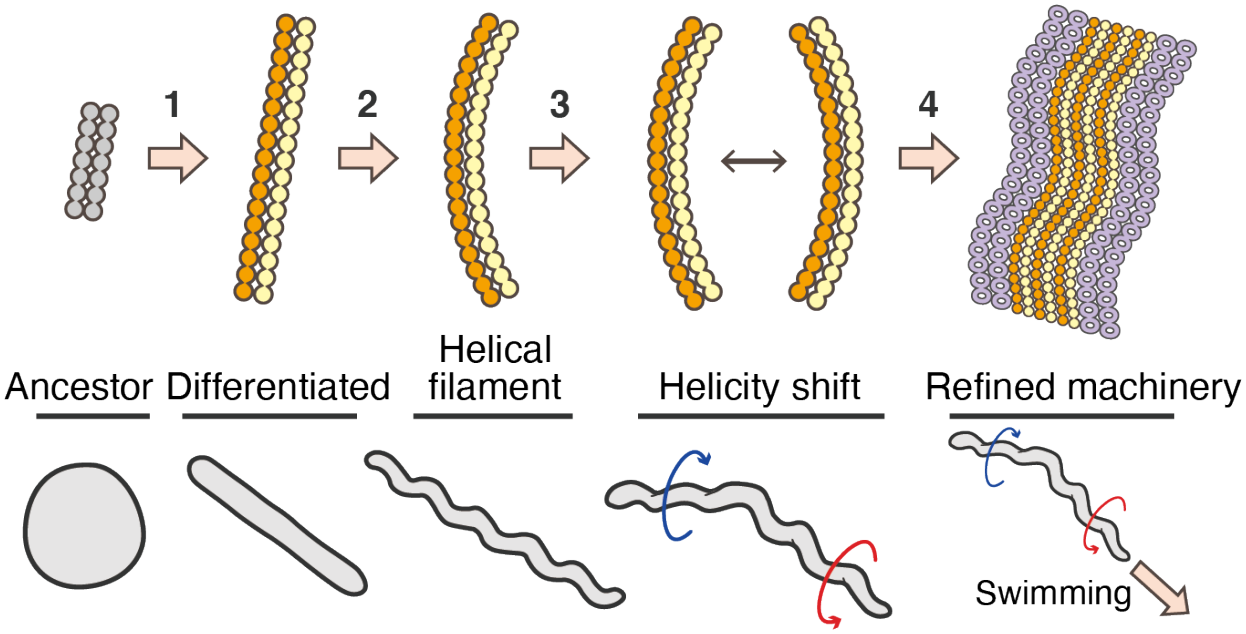

Fig. 4. Schematic for origin and mechanism of Spiroplasma swimming. The swimming mechanism may be acquired through four steps as presented by arrows. Step 1: The MreB protein derived from walled bacteria differentiated into two classes with different characters through accumulated mutations. Association of heterogeneous protofilaments allowed stable filament formation. Step 2: Small differences in length generated curvature, resulting in helicity of the heterogenous filament. Step 3: Change in length caused by ATP energy induces change in curvature, causing helicity switching. The early stage of swimming was acquired. Step 4: The acquired swimming was refined to be equipped by five classes of SMreBs, fibril, dumbbell structure and so on. Corresponding cell morphology and behaviors are presented in the bottom.